IMECE2013-63628

DRAFT: COMPUTATIONAL OPTIMIZATION OF ARC WELDING PARAMETERS USING COUPLED GENETIC ALGORITHMS AND FINITE ELEMENT METHOD

Mohammad R. Islam*
MSU/CAVS
Starkville, MS, USA
mri27@msstate.edu

Jens Rohbrecht
Simufact Engineering GMbh
Hamburg, Germany
jens.rohbrecht@simufact.de

Arjaan Buijk
Simufact-Americas LLC
Plymouth, MI, USA
arjaan.buijk@simufact-americas.com

Ehsan Namazi
University of Winsor
Winsor, ON, Canada
ehgh22@gmail.com

Bing Liu
F.tech R&D North America Inc.
Troy, OH, USA
bliu@ftech-rd.com

Tsuneo Kurosu
F.tech Haga Tech. Center
Tochigi, Japan
tkurosu@ftech.co.jp

Keiichi Motoyama
MSU/CAVS
Starkville, MS, USA
keiichi@cavs.msstate.edu

ABSTRACT

An effective and rigorous approach to determine optimum welding process parameters is implementation of advanced computer aided engineering (CAE) tool that integrates efficient optimization techniques and numerical welding simulation. In this paper, an automated computational methodology to determine optimum arc welding process control parameters is proposed. It is a coupled Genetic Algorithms (GA) and Finite Element (FE) based optimization method where GA directly utilizes output responses of FE based welding simulations for iterative optimization. Effectiveness of the method has been demonstrated by predicting optimum parameters of a lap joint specimen of two thin steel plates for minimum distortion. Three dimensional FE model has been developed to simulate the arc welding process and validated by experimental results. Subsequently, it is used by GA as the evaluation model for optimization. The optimization results show that such a CAE based method can predict optimum parameters successfully with limited effort and cost.

Keywords : Computational Optimization Method, Welding Simulation, Finite Element Modeling, Genetic Algorithms, Computer Aided Engineering (CAE).

1. INTRODUCTION

Arc welding is a major joining process used in every manufacturing industry large or small. It is widely used specially in automotive, aerospace and shipbuilding industries due to its being efficient, economical and dependable as a mean of joining metals. However, welding can introduce significant distortion in final welded geometry which causes loss of dimensional control , costly rework and production delays [1]. In automotive industry, it is a common practice today to use thin sectioned high-strength sheet metals to achieve reduced weight and fuel economy. But the structures made of relatively thin components are the most vulnerable to distortion when subjected to welding. Despite tremendous development in welding technology over the years, weld induced distortion is still one of the major obstacles for cost-effective fabrication of light-weight structures.

Distortion in welded structures is largely influenced by the design parameters of welding process. Better control of these welding variables will eliminate the conditions that promote distortion [2]. But welding is a highly nonlinear multivariate process where several parameters contribute together to produce distortion. Minimization of distortion thus requires simultaneous optimization of multiple input parameters that is often time consuming, costly and not guaranteed to achieve by trial and error based experimental methods. Hence, industrial welding processes today require a robust process design tool to determine optimum set of process control parameters for reduction of weld induced distortion in structures.

The finite element method (FEM) has proven to be a versatile tool of predicting weld induced distortion of welding

---
* Address all correspondence to this author.

processes. Many researchers investigated the generation of welding distortion over the years using FEM. Michalaras and Debiccari [3] applied decoupled 2D and 3D finite element analysis technique to predict welding-induced distortion in large and complex structures. Tsai et al. [2] has investigated distortion mechanism and the effect of welding sequence on panel distortion using FEM based on inherent shrinkage method. Lindgren provided an extensive review on finite element modeling for welding residual stress and distortion prediction in his papers [4-6]. All these works have provided important and useful information about weld induced distortion phenomena. However, the advantage of this knowledge associated with distortion mechanism can be augmented tremendously when FEM based welding simulations will be integrated with numerical optimization techniques to obtain optimum process control parameters. The integration of numerical optimization and welding simulation makes it possible to find optimum parameters computationally with less effort and cost than conventional trial and error based experimental method. In spite of the potential of such integrated optimization system, few research works have been conducted in this arena. Goldak and Asadi [7] have addressed this promising integration aspect and discussed in details the significance of computational optimization for improvement of welding process design. Motoyama [8] has also explained the advantages of simulation based design optimization for welding process.

GA has been extensively used as a mean of performing global optimization in a wide domain of engineering design problems. GA requires only objective function values and thus it can handle optimization problems with discontinuous, non-differentiable or stochastic objective functions. It can also treat discrete and/or continuous design variables allowing greater design flexibility during optimization. As such, it is very suitable for a nonlinear and unorthodox optimization problem like welding process parameter optimization.

In this work, a computational optimization system, which combines FEM based welding simulation and evolutionary optimization method Genetic Algorithms, has been developed. After performing a proof-of-concept optimization to verify integrated system, this approach was successfully applied to a simple lap joint test case. A three dimensional finite element model has been developed and validated by previously conducted experimental results at first. Then , the model was used in optimization. Weld induced distortion has been set as objective function and minimum weld quality requirement has been set as manufacturing constraints. Welding torch speed, input current, arc voltage and welding direction have been set as design variables. The obtained results of optimization have been discussed in this paper.

2. COMPUTATIONAL OPTIMIZATION SYSTEM

The proposed computational optimization system consists of four computer programs- (1) optimization program, (2) welding simulation program, (3) simulation input generation

program and (4) simulation output evaluation program. The structure of the system is illustrated in Fig.1. The four programs are integrated sequentially in a closed loop to establish an automatic and iterative optimization system. The first program is the optimization program which is the main controlling program of the system. It runs GA to produce new population of design variables based on the simulation results of previously evaluated models. It also takes important decision of stopping the analysis by checking the stopping criteria in each iteration. Furthermore, it also keeps records of results, current model information and constraint violations in each iteration. MATLAB® has been used as a programming environment for the entire system algorithm development. The genetic algorithm solver of MATLAB® has been used for optimization.
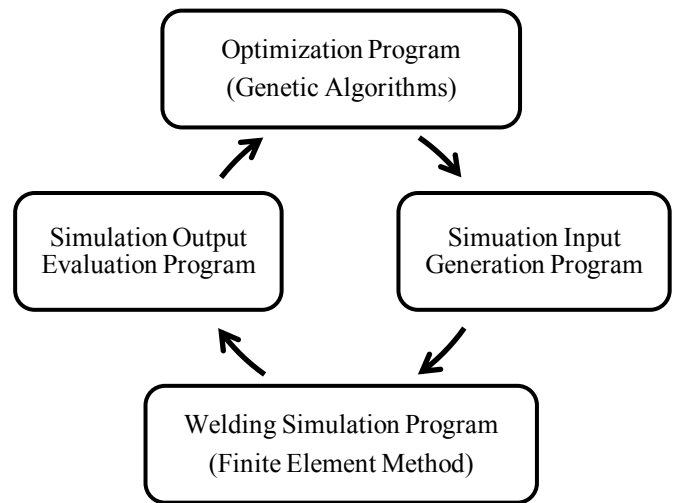

Figure 1. FRAMEWORK OF COMPUTATIONAL OPTIMIZATION SYSTEM.

Simulation input program is the next program which is a simple input-output function. It takes new values of design variables as input, inserts those values into the FEM input file and passes the updated input file to the welding simulation program as output. Welding simulation program is a commercial FE welding simulation program named simufact.welding©. It executes the welding simulations based on input file and stores the desired output results. The last program is the simulation output evaluation program which is a simple text file reading function by nature. It reads the output result files of welding simulations, extracts the specified results and feedbacks the optimization program with those extracted results. The optimization program uses the extracted results to produce new population and in this way the analysis loop repeats until the best solution does not change over pre-specified number of iterations.

3. WELDING EXPERIMENTS

The aim of the experiments was to measure the transient thermo mechanical responses of the welded joint for FE model

validation. It is a single pass welded lap joint specimen. The plate dimensions are 170mm by 35 mm by 3.2 mm and the weld length is 70 mm at the approximate middle section of the plates as shown in Fig. 2. The welding operation was performed using industrial welding robot and the welding parameters used were 20.5 volts, 200 amps and 10 mm/s welding speed.
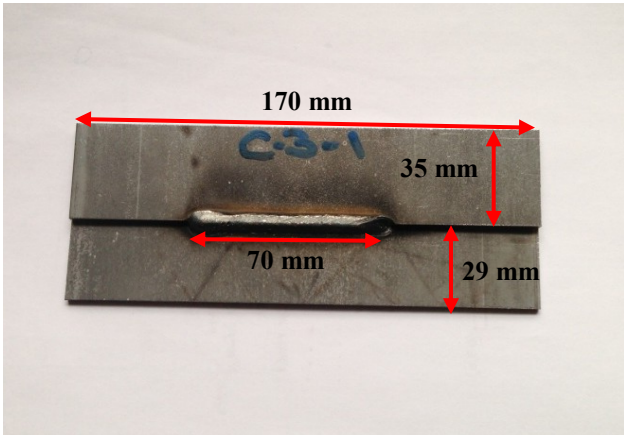

Figure 2. WELDED SAMPLE WITH NECESSARY DIMENSIONS.

The robot had a rotatable table for supporting the specimens and keeping the weld line parallel to the ground level constantly. The welding gun was held by the robot and aside from desired welding directions, it could maintain both up and down, stand-off distance and angular movements for setting the required nozzle-to-plate distance and welding gun angle respectively. A welding gun leading angle of 10 degrees, included angle of 60 degrees and stick out of 12 mm was used in the experiments. Gas mixture of 80% argon and 20% of CO_2 at a constant flow rate of 18 l/min was used to provide an adequate shielding of the weld pool. Before welding, the plates were held in position tightly together by using four spring clamps to prevent movement or separation during welding as shown in Fig. 3.

Figure 3. EXPERIMENTAL SETUP OF THE SPECIMEN.

The material of the plates is ASTM A591M-89 sheet metal steel. Sheet metal steel solid filler wire AWS A5.18-2005 of 0.045 inch diameter was used. The chemical composition of the base metal and fillet metal has been shown in Table 1.

Table 1. CHEMICAL COMPOSITION OF BASE METAL AND FILLET METAL.

Chemical composition in weight %		
Elements	Base Metal	Filler Metal
C	0.173	0.1
Si	0.07	0.04
Mn	0.72	0.95
P	0.011	0.006
S	0.004	0.004
B	0.0002	-
Al	0.044	-
Cr	0.05	0.02
Mo	0.004	0
Ni	0.02	0.02
Cu	0.05	0.17

After welding experiments, the welding macro tests were performed to investigate primarily presence of defects, weld pool shape and depth of weld penetration. The macro samples were prepared by sectioning a test weld, polishing the cut surface smooth and bright and then etching with a suitable reagent. The tests were performed and repeated in three different areas of start, middle and at the end cross section of the samples along the welding path. A macrograph of the weld cross-sectional view of the specimen (at 35 mm depth from starting point) is shown in Fig. 4.
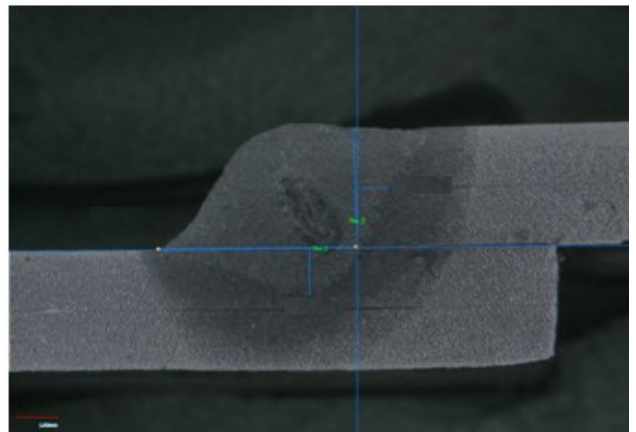

Figure 4. MACROGRAPH OF WELD CROSS SECTION.

Visual inspection of experimental welding samples reveals that both upper and lower plates underwent primarily out-of-plane distortion in z direction for welding. A laser scanner was used to measure the z-directional distortion in the part. However, in-plane distortion could not be measured. While scanning, the scanner has captured thousands of data points over the top

surface of welded specimens. For distortion calculation, the captured data point cloud was compared to a reference model. The reference model was just two plates glued together. The measurements were then processed and reported in the form of graphical data represented by contour plots. The experimental distortion results have been shown in next chapter.

4. WELDING SIMULATION

Two dimensional models have been predominantly used in the most of the earlier studies of welding simulation. However, three dimensional FE models are required for distortion prediction because the effect of two dimensional constraints are quite larger for quantities like deformation and strain [5].

4.1 Finite Element Modeling

The modeling has been initiated by generating the model geometries in a suitable CAD system and then the geometries were meshed precisely. The complete three dimensional finite element model has been shown in Fig. 6(a) and weld pool shape has been shown in Fig. 6(b).
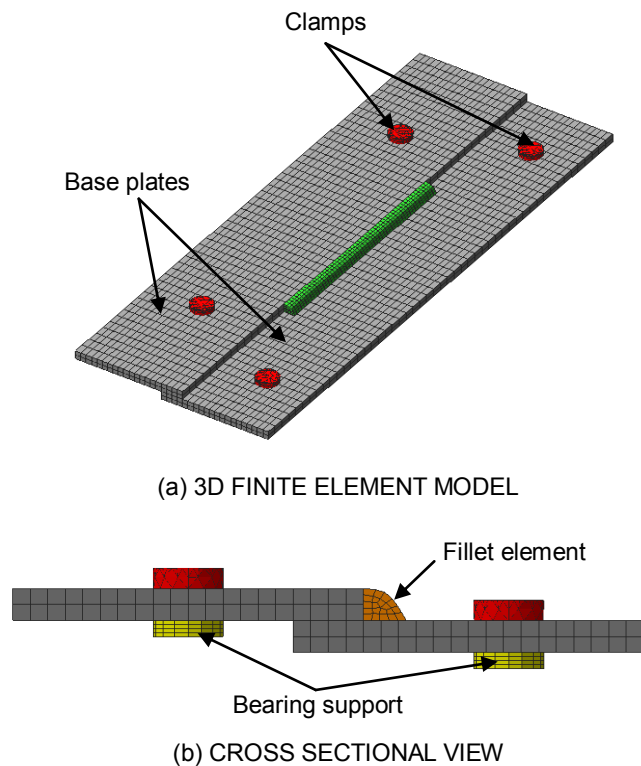

(a) 3D FINITE ELEMENT MODEL

(b) CROSS SECTIONAL VIEW

Figure 6. DETAILS OF FINITE ELEMENT MODEL.

The entire FE model consists of eleven geometries- two geometry to represent the base plates, one geometry for fillet metal and the rest of them for representing the boundary conditions. We have used four bearing supports and four clamping tools as boundary conditions. Four clamps were positioned exactly at the same positions just like the

experimental setup on the top surfaces of the plates and they were released during cooling process to allow stress relief and distortion. The holding force of each clamp was equal to 500 N. The bearing supports were placed exactly at the same positions of the clamps but on the bottom surfaces of plates as shown in Fig.6(b). All the geometries corresponding to boundary conditions are treated as rigid bodies during simulation and they are made of only thermal elements. As thermal boundary conditions, heat transfer due to convection, radiation and contact with fixtures have been considered. The relevant parameters have been given in Table 2.

Table 2 HEAT TRANSFER COEFFICIENTS.

Coefficient name	Value
Convective heat transfer coefficient, h	20 W/m^2.K
Contact heat transfer coefficient , α	100 W/m^2.K
Emission coefficient , ϵ	0.6

The model contains 6560 eight noded hexagonal elements and 10347 nodes. Each base plate consists of 2720 elements and the fillet material consists of 1120 elements. The initial model was coarse in mesh as adaptive meshing has been implemented to refine the mesh in the vicinity of weld path by splitting the original existing elements during analysis. A refinement level of 2 has been used and heat source area has been treated as refinement criterion. As such, the initial fillet metal element size along the weld path was 1.25 mm but during analysis the element size was reduced to 0.3125 mm by refinement. The criterion is set by means of a scaling factor which is a multiplier of the heat source size for the local refinement area around the heat source. A scaling factor of 2 has proven to be reasonable for achieving accurate molten zone shape by simulation.

A double ellipsoid heat source, first proposed by Goldak et. al [9], has been used to simulate the arc welding heat input. The heat source dimensions have been adjusted to obtain the correct heat flux input and correct shape of the melted zone. The heat source parameters has been shown in Table 3.

Table 3 HEAT SOURCE PARAMETERS.

Power (W)	4100
Efficiency	80 %
Front Length, a_f (mm)	1.0
Rear Length, a_r (mm)	1.5
Width , b (mm)	3.5
Depth, d (mm)	4.0
Heat Front Scaling Factor	0.4

Three-dimensional thermo-mechanical FEM simulations were carried out using Marc solver of simufact.welding©. Marc uses a staggered solution procedure in coupled thermo-mechanical analysis where It first performs a heat transfer analysis, then a stress analysis. The dynamic creation of fillet material has been achieved by the deactivated element method

where elements are first deactivated along the weld path, then revived as the moving heat source takes position within the elements. The material model used in the simulation included relevant temperature dependent thermal and mechanical properties as illustrated in Fig. 7(a) and Fig. 7(b) respectively.
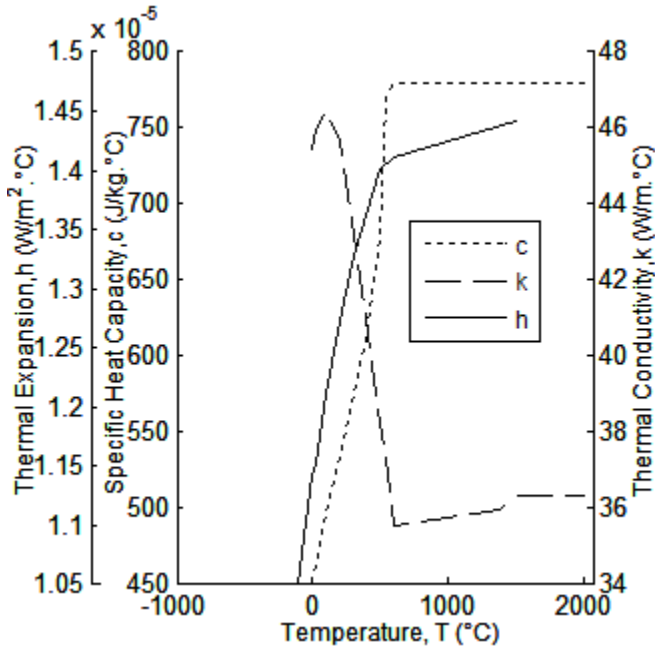
(a) Thermal properties
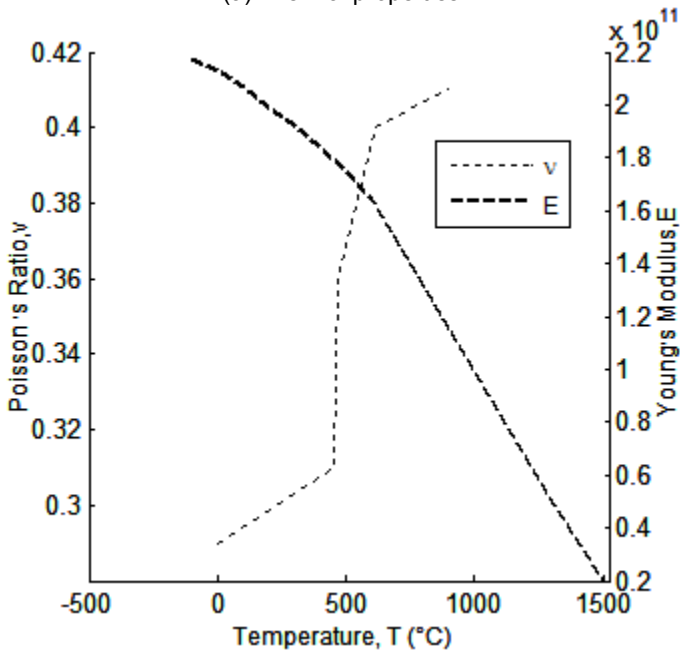
(b) Mechanical properties

Figure 7. TEMPERATURE DEPENDENT MATERIAL PROPERTIES.

4.2 Simulation Results

The computational time required to run the complete thermo-mechanical simulation was approximately five hours and was performed on a 2.30 GHz Intel (R) Core(TM) i5-2410M CPU with 8 GB ram. The total simulation time was 157s in which welding time was 7s and cooling time was 150s. A cooling period of 150s was sufficient because distortion did not vary significantly after this time period. The main driving force in welding simulation is heat generation process. Thus, to predict the behavior of a weld in a structure, the transient temperature field driven by the weld heat source must be computed with useful accuracy [10]. In this work, the heat source model or temperature field has been validated with respect to the weld macrographs of experimental weld cross sections and a fairly good agreement has been achieved in terms of weld pool fusion zone shape and size as illustrated in Fig. 8.

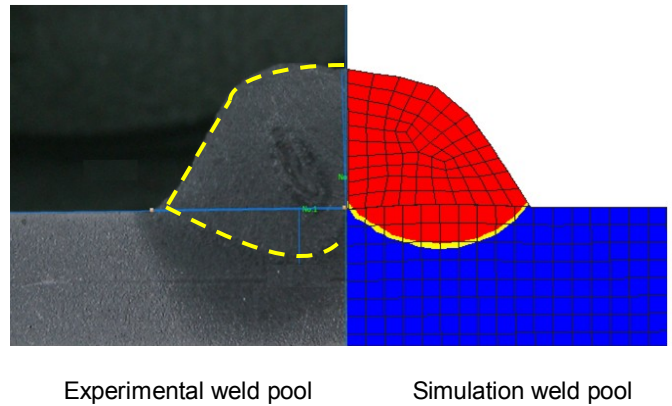Experimental weld pool   Simulation weld pool

Figure 8. MEASUREMENT OF WELD POOL SHAPE.

The typical simulation predicted temperature field across the cross section of the weld bead can be seen in Fig. 9. The figure confirms good welding quality since the temperature of the weld pool is above material melting point temperature (1500 °c).
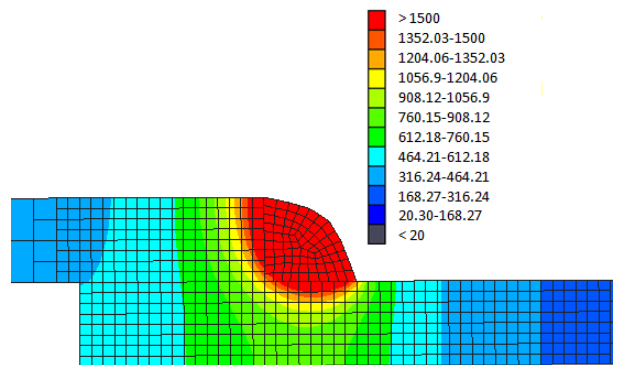

Figure 9. TEMPERATURE FIELD ACROSS WELD CROSS SECTION (TIME= 3.5s).

After validating the heat source, the simulation predicted out-of-plane distortion was compared with experimental results by contour plots. Figure 10 shows the contour plot of experimental out-of-plane distortion. The maximum positive distortion has occurred at the middle section along the edge of the lower plate (Fig. 10) and its magnitude is 0.53 mm. The maximum negative bending is 0.401 mm. Figure 11 shows the bending distortion pattern predicted by welding simulation. The maximum bending distortion obtained by simulation was 0.49 mm and 0.35 mm respectively in positive and negative z axis. The comparison of contour plots indicates that almost similar out-of-plane distortion pattern has been achieved by welding simulation and experiments. But a quantitative comparison is not possible through these contour plots. However, for optimization purpose, it is sufficient to predict general distortion trend and magnitude with good accuracy.
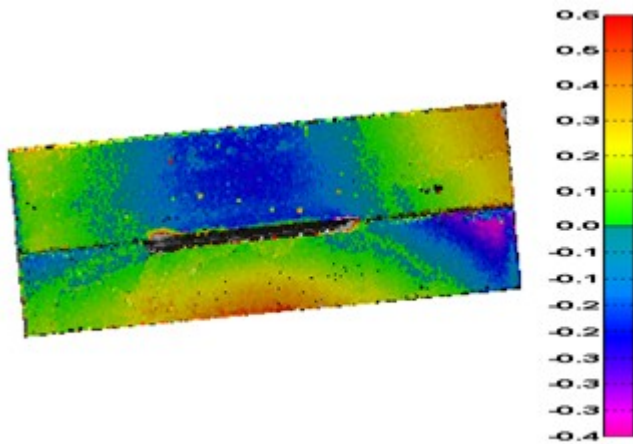

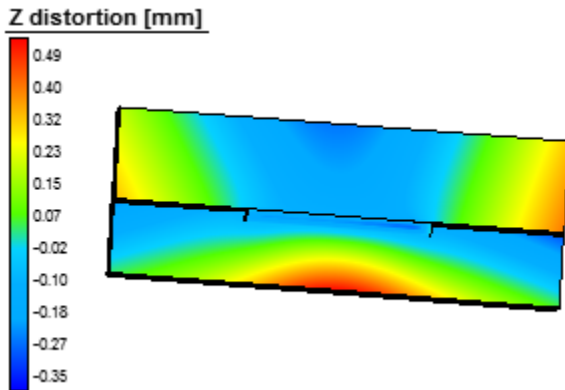**Figure 10. EXPERIMENTAL OUT-OF-PLANE DISTORTION (in mm unit).**

Figure 11. SIMULATION PREDICTED OUT-OF-PLANE DISTORTION.

Furthermore, total distortion pattern obtained by simulation has been shown in Fig. 12. The total distortion prediction by simulation also confirms that out-of-plane distortion (z axis) is the main contributing factor for distortion in the structure. Maximum distortion (0.50 mm) has occurred at middle section of the lower plate as well.
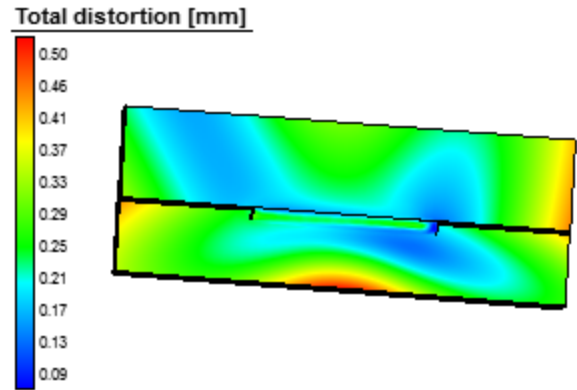

Figure 12. SIMULATION PREDICTED TOTAL DISTORTION.

5. GENETIC ALGORITHMS BASED OPTIMIZATION

Genetic Algorithms can be considered as a controlled random walk, they efficiently exploit information from previous configurations to generate new configurations with improved performances expected [11]. It starts search with an initial set of random solutions called population. Each individual in the population is a solution to the optimization problem. The individuals evolve through successive iterations, called generations, mimicking the process of natural evolution. Through this evolution process, the algorithm actually searches for better solutions. During each generation, the individuals are evaluated using some measure of fitness. To explore new design points, new individuals are formed by modifying less fit individuals by genetic operators. After several iterations, the algorithm converges to the best solution, which is assumed to represent the optimum solution of the problem.

5.1 Optimization Problem Formulation

In this paper, the goal is to reduce the weld induced distortion. Through welding simulation, total distortion in all nodes (N) has been first calculated as the sum of square roots of nodal distortions in all three direction. Then, maximum distortion value has been found out and used as objective function value for iterative optimization via GA. Thus, the objective function definition is given by Equation 1.

$$F(X) = \max(D_i) \qquad\qquad (1)$$
$$D_i = \sqrt{(d_x)^2 + \left(d_y\right)^2 + (d_z)^2} \quad i = 1,2,3 \dots N$$

Welding speed (X1), arc voltage (X2), input current (X3) and welding direction (X4) have been set as design variables. Design variables have been treated as discrete valued variables. The design variables except welding direction can take four discrete numeric values. Details of design variables have been shown in Table 4.

Copyright © 2013 by ASME

Table 4. DESIGN VARIABLE DEFINITION.

Design Variable	Unit	Lower Bound	Upper Bound	Discrete Values
X1	mm/s	3.5	10	3.5,5,7,10
X2	Volt	10	30	10,15,20,25
X3	Amp	100	250	100,150,200,250
X4	-	-	-	1,2,3,4,5,6

Design variable defining welding direction can take six numerical value to represent six possible welding directions as shown in Table 5. Two welding directions are designed with one robot and they have been represented by integer value 1 and 2 respectively depending on robot's left-right or right-left movement direction. Similarly, the remaining four welding directions are designed with two robots and they have been represented by a integer from 3 to 6 depending on each robot's left-right or right-left movement direction. for two robot welding cases, it was assumed that both robots will start and stop welding at the same time.

Table 5. DEFINITION OF WELDING DIRECTION VARIABLE.

Value	Welding Direction Symbol	No. of Robots	Starting Timing
1	⟶	1	Same
2	⟵	1	Same
3	- - - - ▸◂ ⟵	2	Same
4	◂ - - - ⟶	2	Same
5	- - - - ▸ ⟶	2	Same
6	◂ - - - ◂ ⟵	2	Same

During optimization process, GA picks design variables automatically. As such it is very likely that it will often pick design variables that will result in poor welding quality. If the heat input parameters are very low, welding quality will be poor due to incomplete fusion or insufficient weld penetration. To ensure a strong welding joint and good quality, it is important that the temperature around the welding zone is higher than or equal to melting temperatures of base metals and fillet metals during welding. As such temperature constraints have been used to ensure good weld quality. During finite element simulations, temperatures at three different fillet metal cross sections have been monitored to check temperature constraint. The tracking sections are at 10mm,35mm and 60mm distances respectively from starting point. To incorporate the constraint violation into optimization algorithm, a penalty term is added to the objective function and the combined function is called augmented function. Whenever a constraint is violated, the penalty term is greater than zero, with the magnitude of the penalty being proportional to severity of constraint violations. In this work, the penalty term is proportional to the number of sections (N_c) that has violated the constraint. The augmented objective function definition including optimization constraints is given by Equation 2.

$$\varphi(x) = \begin{cases} F(X), & N_c = 0 \\ F(X) + 100 * N_c, & N_c > 0 \end{cases} \quad (2)$$

The penalty term increases the original objective function value and indicates GA the associated model is infeasible. An infeasible model represents poor welding quality even though the weld induced distortion may be small.

5.2 Implementation of GA

The arc welding optimization approach using genetic algorithm has been shown in Figure 13. It initiates GA by creating a random initial population and each individual of the initial population is evaluated by the FEM tool. In this work, an individual represents a set of Welding speed (X1), arc voltage (X2), input current (X3) and welding direction (X4).
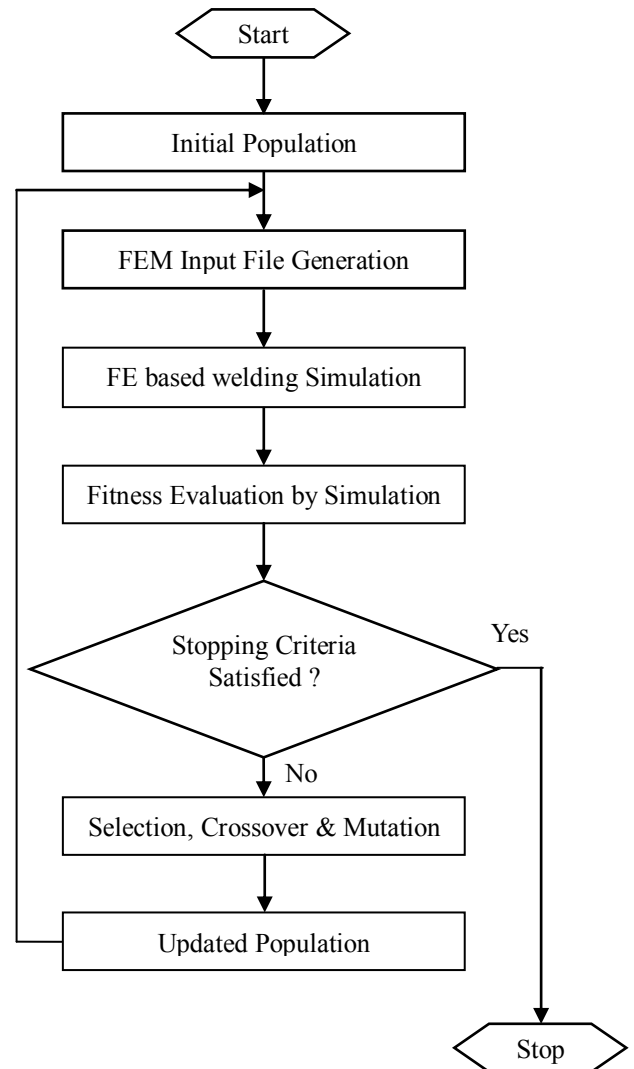

Figure 13. GA-FEM COUPLED OPTIMIZATION ALGORITHM.

Then based on the augmented function values obtained from simulation output evaluation program, GA creates next generation and reevaluates this population using FEM tool. The program stores each individual and its fitness value so as to ensure not to reevaluate twice the same individual in successive generations. The system algorithm runs until maximum number of generations have been reached or the cumulative change in the objective function value over five generations is less than or equal to objective function tolerance.

In this work, to optimize the welding parameters, GA was directly linked with simulation model. Considering the simulation time required for a refined model, less refined model has been implemented in optimization. The model refinement is critical in predicting the weld pool phenomena but the refinement effect is nominal for distortion prediction. Although FEM is computation intensive tool, one can still perform distortion simulations with an acceptable accuracy using a simplified heat source and material description [12].

6. OPTIMIZATION RESULTS
The optimization results have been illustrated in Table 6. It can be seen that optimization of process parameters was successful in reducing the maximum weld induced distortion. The maximum total distortion obtained with optimum parameters is 0.4431 mm. The maximum out-of-plane distortion (z distortion) obtained with optimum parameters is 0.4179 mm which is 21.15% less than experimental maximum out-of-plane distortion (0.53 mm). Furthermore, it is seen that optimum heat input is 2250 W which is just 54.87% of experimental heat input (4100 W). A reduced weld speed and the weld robot trajectory segmentation into two portions was proven to be effective in reducing weld distortion.

Table 6. OPTIMIZATION RESULTS.

X1 (mm/s)	X2 (V)	X3 (A)	X4	Max. Distortion (mm)	Max. Z Distortion (mm)
7	15	150	5	0.4431	0.4179

Figure 14 shows the optimization result convergence history with respect to the calculation generations or iterations. The convergence history also reveals that z-directional or out-of-plane distortion is the dominant part of total distortion and it is the most sensitive to the change in considered design variables. The optimization converged with around 11 iterations and at the cost of maximum 53 FE simulations.
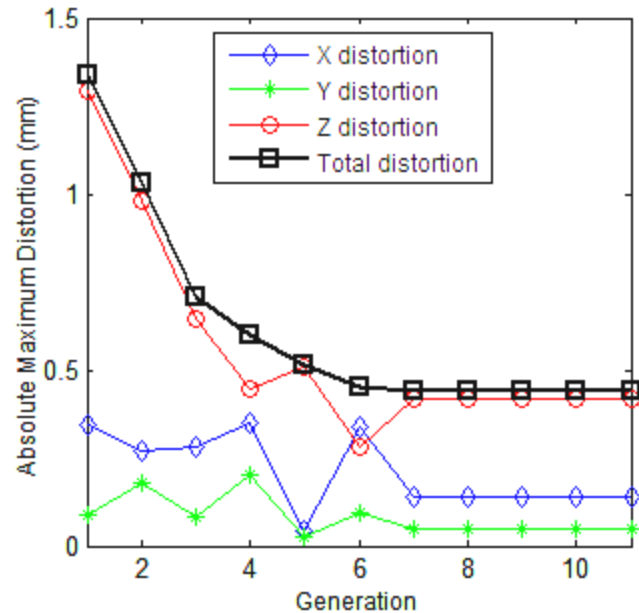

Figure 14. OPTIMIZATION RESULT CONVERGENCE HISTORY.

7. CONCLUSION
Automated design optimization of welding process based on integrated CAE tools can contribute substantially to enhance final welded product, to facilitate and accelerate the product design and development. This study introduces a simple computational framework based on commercial CAE tools which allows automatic optimization of process parameters without the requirement of expensive trial experiments. The system is also capable of exploring a wide domain of design variables with limited modification in simulation model. Thereby, possibility of finding the most optimum process parameters is higher in this method.

The illustrative example presented shows that the proposed GA-FEM coupled method is able to search for optimum set of process parameters specially under the critical constraint of weld quality requirement. In the current optimization problem, an straightforward solution approach is to run all possible 368 (4x4x4x6) combinations and select the best one as optimum solution. However, it will be computationally inefficient and sometimes infeasible considering the extensive computational time required for FE simulation. Using GA, we achieved optimum results with only 53 FE simulations. So, the method is certainly effective for this case study. However, since GA is a deterministic algorithm, it may not be efficient and feasible for other case studies with more complex models. As such more studies, specially with complex structures need to be conducted. Besides, metamodeling technique to substitute computation intensive simulations can be integrated to make the methodology more versatile and robust. Consideration of additional design variables such as clamping position, clamp

apply/release time and weld sequencing will be the objects for future research.

ACKNOWLEDGMENTS

REFERENCES

[1] Michaleris, P., 2011, Minimization of Welding Distortion and Buckling, Woodhead Publishing, pp. 3.

[2] TSAI, C. L., PARK, S. C. and CHENG, W. T., 1999, "Welding Distortion of Thin-Plate Panel Structure," Welding Research Supplement, pp. 156-164.

[3] Michaleris, P., and Debiccari, A., 1997, "Prediction of welding distortion," Welding Journal, 76(4) , pp. 172-179.

[4] Lindgren, L.-E., 2001, "Finite Element Modeling and Simulation of Welding, Part 1: Increased Complexity," Journal of Thermal Stresses, 24, pp. 141-192.

[5] Lindgren, L.-E., 2001, "Finite Element Modeling and Simulation of Welding, Part 2: Improved Material Modeling," Journal of Thermal Stresses, 24, pp. 195-231.

[6] Lindgren, L.-E., 2001, "Finite Element Modeling and Simulation of Welding, Part 3: Efficiency and Integration," Journal of Thermal Stresses, 24, pp. 305-334.

[7] Goldak, J. and Asadi, M., 2011,"Computational Weld Mechanics and Optimization of Welding Procedures, Welds and Welded Structures," *Transactions of JWRI, Special Issue on WSE2011*, Osaka, Japan, pp. 55-60.

[8] Motoyama, K., 2010, "Implications of Welding Simulation Techniques to Optimize Manufacturing Processes," Technical Presentation, DETC2010-29105, ASME 2010 International Design Engineering Technical Conferences and Computers and Information in Engineering Conference , Montreal, Canada.

[9] Goldak, J., Chakravarti, A. and Bibby, M., 1984, "A New Finite Element Model for Welding Heat Sources," Metallurgical Transactions B, 15B, pp. 299-305.

[10] Goldak, J. A., and Akhlagi, M., 2005, Computational Welding Mechanics, Springer, New York , pp. 79, Chap. 3.

[11] Goldberg, D. E., 1989, Genetic Algorithms in Search, Optimization & Machine Learning, Addison-Wesley, Massachusetts, Chap. 1.

[12] Lundback, A., 2003, "Finite Element Modeling and Simulation of Welding of Aerospace Components," Ph.D. thesis, Lulea University of Technology.